ISSN 2564-3258

RESEARCH ARTICLE

X-Ray Interaction Cross-Sections and Scattering Coefficients of $_{21}Sc^{45}$, $_{25}Mn^{55}$, $_{31}Ga^{70}$, $_{56}Ba^{137}$, and $_{78}Pt^{195}$ for Applications in Radiation Shielding and Radiology

Hunain Maqbool[1], Wardah Naim[2], Muhammad Maqbool[3*]

Maqbool H, Naim W, Maqbool M. X-Ray Interaction Cross-Sections and Scattering Coefficients of $_{21}Sc^{45}$, $_{25}Mn^{55}$, $_{31}Ga^{70}$, $_{56}Ba^{137}$, and $_{78}Pt^{195}$ for Applications in Radiation Shielding and Radiology. Int J Radiol Case Rep. 2025;2(1):17-27.

Abstract

One of the most successful ways of treating cancer and malignant tumours is radiation. Most of the radiological and diagnostic processes are also possible due to the use of radiation. However, it is important to protect radiation workers using various shielding materials due to the hazards associated with high-energy radiation. In addition, the quality of radiological images is also affected by the energy and intensity of radiation used in the imaging process. The use of shielding material is more productive in radiological imaging, only if its basic characteristics, properties, and interaction with radiation are studied. The purpose of the present work is to use the Klein-Nishina formula to calculate the electronic cross-sections, atomic cross-sections, energy-transfer cross-sections, and compton scattering coefficients of Scandium ($_{21}Sc^{45}$), Manganese ($_{25}Mn^{55}$), Gallium ($_{31}Ga^{70}$), Barium ($_{56}Ba^{137}$), and Platinum ($_{78}Pt^{195}$) when X-rays or γ-radiation interact with these elements. The results show that the Klein-Nishina cross-section per electron and Klein-Nishina cross-sections per atom decrease with increasing photon energy and increase when the charge number Z of the elements is increased. The compton Scattering coefficients also decrease for highly energetic radiation and increase with the ratio of charge number Z and mass number A of an element. Thus, it is recommended that compton scattering coefficients should not be studied as a function of Z or A separately, but instead as a function of Z/A. The results also conclude that the investigated materials can be used for applications in radiation shielding, dosimetry, and radiological imaging.

Key Words: *X-rays; Radiation shielding; Radiological imaging; Klein-Nishina cross-sections; Compton coefficients*

[1]*Hoover High School, 1000 Buccaneer Dr, Hoover, AL 35244, USA*

[2]*Vestavia Hills High School, 2235 Lime Rock Rd, Vestavia Hills, AL 35216, USA*

[3]*Department of Clinical and Diagnostic Sciences, University of Alabama , Birmingham, AL 35294-1212, USA*

[*]*Corresponding author: Muhammad Maqbool, Professor, Department of Clinical & Diagnostic Sciences, University of Alabama, Birmingham. AL 35294-1212, USA, E-mail: mmaqbool@uab.edu*

Received: March 06, 2025, Accepted: April 28, 2025, Published: May 19, 2025

This open-access article is distributed under the terms of the Creative Commons Attribution Non-Commercial License (CC BY-NC) (http://creativecommons.org/licenses/by-nc/4.0/), which permits reuse, distribution and reproduction of the article, provided that the original work is properly cited and the reuse is restricted to noncommercial purposes.

Introduction

Cancer is a growing problem worldwide. In 2022, the World Health Organization reported that there were an estimated 20 million new cancer cases and 9.7 million deaths in the world [1,2]. Human exposure to radiation with an acute dose of as low as 10 mSv to 50 mSv can increase the risk of cancer [3-7]. Accidental exposure to higher doses can bring more hazards and adverse effects that can cause complications in human health [8,9]. The damaging effects of radiation are diverse and need an in-depth investigation. X-rays have been widely used in cancer treatment. Despite the enormous benefits of radiation in cancer treatment, excessive radiation exposure is dangerous and can cause cancer. Therefore, shielding and protecting normal tissues from radiation is equally important for a radiation worker or a patient being exposed to radiation during diagnosis or treatment using radiation [10-12]. These alarming data and reports show that more efficient ways of preventing cancer are needed. One of the important and effective ways to achieve this goal is to use various materials for radiation shielding within hospitals and radiation working areas anywhere [13-15]. Moreover, the use of a proper shielding material controls the intensity and energy of the interacting radiation used in radiological imaging, which results in improved image quality [10,11].

Shielding material, in general, refers to the placement of absorbent material or attenuator between people and radiation sources, which can attenuate the radiation beam enough to provide not more than background radiation to the exposed people [16-18]. An absorber can be any material that reduces the spread of radiation from the source and protects a radiation worker from overexposure to radiation because, as radiation, like X-rays, passes through matter, the intensity of that radiation is diminished [19,20]. Because of the importance of shielding materials, it is mandatory to understand the properties and radiation shielding ability of these materials and their applicability and use in radiation protection [8,21]. Investigating the characteristic properties of these materials will help in dose calculation an daccurac yin radiatio ndosimetr yan dradiation oncology [16-22].

Compton scattering is an important interaction to consider when determining the shielding ability of materials. Different calculations are needed to determine the cross-sections and scattering, and attenuation coefficients. The mass attenuation coefficient represents how much energy is lost to absorption and scattering after interaction with an atom. The ideal scenario is to have a shielding material that absorbs most of the energy and causes very little scattering [23,24].

The present work reports the use of Gamma rays or X-rays of energies 364 keV, 1.25 MeV, 4.784 MeV, 6 MeV, 9 MeV, and 18 MeV to study and investigate Scandium ($_{21}Sc^{45}$), Manganese ($_{25}Mn^{55}$), Gallium ($_{31}Ga^{70}$), Barium ($_{56}Ba^{137}$), and Platinum ($_{78}Pt^{195}$) for their use as radiation shielding materials, using Klein-Nishina formula. The Klein-Nishina formula is a useful mathematical equation that can be used to calculate the attenuation, absorption, and scattering properties of various materials interacting with photon beams [25-27]. The electronic and atomic cross-sections, mass attenuation coefficients, and mass-energy transfer coefficients of the mentioned materials have been calculated. to find their suitability for radiation shielding and protection purposes. The effect of charge number and the ratio of charge number to mass number on the shielding ability of these materials has also been investigated,

and their values are given in Table 1. In radiation dosimetry and radiation oncology treatment of tumors, it is important to know if the exact prescribed dose is received by a tumour. Klein-Nishina (K-N) cross-sections, compton mass attenuation coefficients, and mass-energy transfer coefficients are among the key factors that calculate the precise dose and quantity of radiation by tissue or part of the body [23,24]. Thus, the present work provides important information about radiation doses in dosimetry processes. In radiation dosimetry and radiation oncology treatment of tumors, it is important to know if the exact prescribed dose is received by a tumour. Klein-Nishina (K-N) cross-sections, compton mass attenuation coefficients, and mass-energy transfer coefficients are among the factors that calculate the precise dose and quantity of radiation by tissue or part of the body [25-28].

TABLE 1
The effective charge number Z and mass number A of materials.

Element	Charge number Z	Mass number A	Z/A
$_{21}Sc^{45}$	21	45	0.4667
25Mn55	25	55	0.4545
31Ga70	31	70	0.4429
56Ba137	56	137	0.4088
78Pt195	78	195	0.4

Materials and Methods

The Klein-Nishina scattering formula is used to calculate electronic cross-sections, atomic cross-sections, compton mass attenuation coefficients, electronic mass-energy transfer cross-sections, atomic mass-energy transfer coefficients, and compton mass-energy transfer coefficients. The Klein-Nishina differential formula is given below [29,30].

$$\frac{d\sigma}{d\Omega}=\frac{r_0^2}{2}\left[\frac{1}{1+\alpha(1-\cos\theta)}\right]^2\left[1+\cos^2\theta\right]\left[1+\cos^2\theta+\frac{\alpha^2(1-\cos\theta)^2}{1+\alpha(1-\cos\theta)}\right](m^2/Sr) \qquad (1)$$

To calculate the total electronic cross-section σ_e, we write $d\Omega = 2\pi.\mathrm{Sin}\theta.d\theta$

The total electronic cross-section σ_e is obtained by solving the Klein-Nishina differential formula of equation (1) and using the equation

$$\sigma_e = 2\pi\int\frac{d\sigma}{d\Omega}.\sin\theta.d\theta \qquad (2)$$

Putting equation (1) in equation (2) and solving, we get the total electronic cross-section, which is given below [29-31].

$$\sigma_e = 2\pi r_0^2\left\{\frac{1+\alpha}{\alpha^2}\left[\frac{2(1+\alpha)}{1+2\alpha}-\frac{1n(1+2\alpha)}{\alpha}\right]+\frac{1n(1+2\alpha)}{2\alpha}-\frac{1+3\alpha}{(1+2\alpha)^2}\right\} \qquad (3)$$

α is the coupling constant, solved by using, $\alpha = \frac{h\nu}{m_0 c^2}$,

where hv is the energy of the interacting photon and is expressed in MeV, and $m_0 c^2 = 0.511 MeV$.

The r_0 is related to the classic radius of an electron and was calculated using.

$$r_0 = \frac{e^2}{m_0 c r^2} = 2.818 x 10^{-13} cm$$

Klein-Nishina atomic cross-sections are obtained by multiplying electronic cross-sections with the charge number Z of each element, using $\sigma_a = Z.\sigma_{e,}$ and the compton mass attenuation coefficient is calculated using.

$$\frac{\sigma}{\rho} = \frac{{}^{N}A^{Z}}{A}\sigma_e$$

The Klein-Nishina transfer cross-section equation was also derived from Equation (1). The equation to find electron transfer cross-sections is below [29,30]:

$$\sigma_e^{tr} = 2\pi r_0^2 \left[\frac{2(1+\alpha)^2}{\alpha^2(1+2\alpha)} - \frac{1+3\alpha}{(1+2\alpha)^2} - \frac{(1+\alpha)(2\alpha^2-2\alpha-1)}{\alpha^2(1+2\alpha)^2} - \frac{4\alpha^2}{3(1+2\alpha)^2} - \frac{4\alpha^2}{3(1+2\alpha)^3} - \left(\frac{1+\alpha}{\alpha^3} - \frac{1}{2\alpha} + \frac{1}{2\alpha^3}\right) ln(1+2\alpha) \right]$$

X-rays or γ-ray energies of 364 keV, 1.25 MeV, 4.784 MeV, 6 MeV, 9 MeV, and 18 MeV were used in the calculations. These energies of X-rays were chosen due to their regular use in diagnostic and therapeutic applications [27-32].

Results and Discussion

Figure 1(a) shows changes in the coupling constant (α) when the energy (E) of the X-ray photon changes. The straight line in the figure shows a linear relationship between the energy and α. Table 1 gives numeric values of the coupling constants for the photon energies used in this work. To study variation in the Klein-Nishina cross-section per electron as a function of X-ray energy, the calculated cross-sections are plotted against X-ray energies. The Klein-Nishina cross-section per electron represents the interaction probability of a photon with a single free electron. Figure 1(b) shows that varies as a function of X-ray energies. This probability establishes the basics of X-ray interaction with matter. The figure shows that within the energy range 0.364 MeV to 18 MeV, the Klein-Nishina cross-section per electron decreases with increasing photon energy.

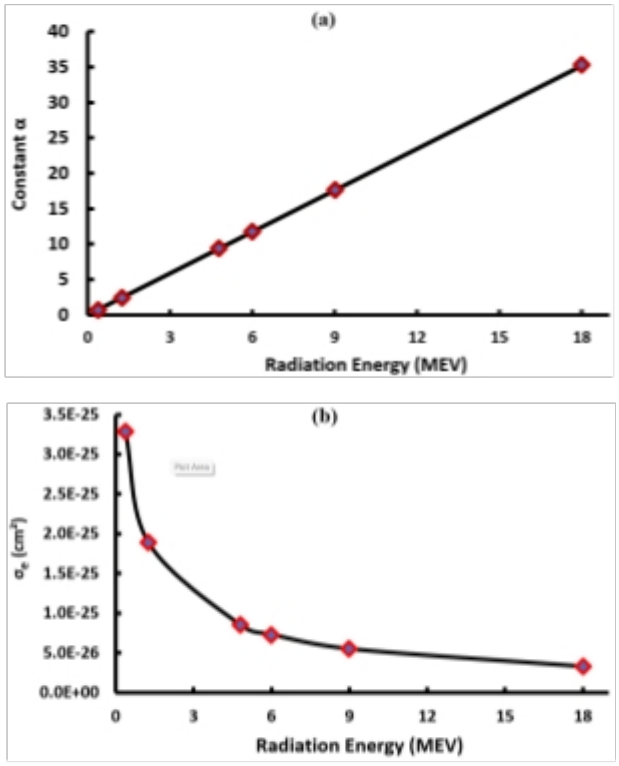

Figure 1). (a) *Increase in coupling constant with increasing X-ray energy, (b) Variation in the Klein-Nishina cross-sections per electron σ_e as a function of X-ray energy.*

Figure 2 shows the Klein-Nishina atomic cross-section for $_{21}Sc^{45}$, $_{25}Mn^{55}$, $_{31}Ga^{70}$, $_{56}Ba^{137}$, relationship between E and can be explained based on various interaction mechanisms of photons with atoms and matter. Compton scattering is the dominant interaction process in the 0.364 to 18 MeV range, followed by pair production and some photoelectric absorption [21,24,27]. In general, the higher the photon energy, the greater the penetration depth achieved by the photon, which indicates fewer chances of interaction with an electron and hence a reduction in the Klein-Nishina cross-section per electron. Table 2 shows the data and numeric values for α and and $_{78}Pt^{195}$.

TABLE 2
Klein-Nishina electron cross-section and electron energy-transfer cross-section as a function of photon energy.

Energy (MeV)	Alpha (α)	Klein-Nishina electronic cross-section eσ (cm2/e)	K-N electron energy-transfer cross section (cm2/e)
0.364	0.71233	32.8547x10-26	9.793x10-26
1.25	2.44618	18.8732x10-26	8.895x10-26
4.784	9.36204	8.53305x10-26	5.328x10-26
6	11.74168	7.32191x10-26	4.719x10-26
9	17.81252	5.50298x10-26	3.727x10-26
18	35.22505	3.28079x10-26	2.375x10-26

The figure gives information about variation in σ_a with photon energy in the 0.364 to 18 MeV energy range and the charge number Z of each element. The Klein-Nishina atomic cross-section provides information about the interaction probability of an X-ray with a single atom through scattering phenomena. Since each atom or element has Z electrons, may be calculated by multiplying by the charge number Z of the atom. The figure shows that increases with increasing charge number Z of the atom, with a minimum of Z=21 for scandium and a maximum of Z=78 for platinum. The reason for this increasing with Z can be attributed to the fact that the lower Z of an atom like $_{21}Sc^{45}$ means a small number of electrons per unit atom, which makes the probability of interaction with a single electron low. On the other hand, many electrons per unit atom, like $_{78}Pt^{195}$ with a high Z, make the probability of interaction with a single electron high. As the number of electrons increases, the chance of interaction also increases. Figure 2 also shows the response of to the changing value of radiation energy. The probability of radiation interaction with an atom decreases as the energy of the photon increases, due to compton scattering, reduced at higher energies, dominated by the phenomenon of pair production in which the absorption of an X-ray occurs. At energies approximately above 12 MeV, the cross-section is minimal due to the dominant pair production at these energies. Overall, Figure 2 shows us how varies as a function of Z and E simultaneously. The figure makes it clear that increases as Z increases, therefore, radiation will have more chances of interaction with a high Z material as compared to a low Z material. In other words, materials with high values of Z will provide better shielding and protection from X-rays. On the other hand, radiation with high energy has less chance of interaction with an atom, and hence

it is difficult to control and shield this radiation. Therefore, big challenges will be faced to shield from X-rays with high energy.

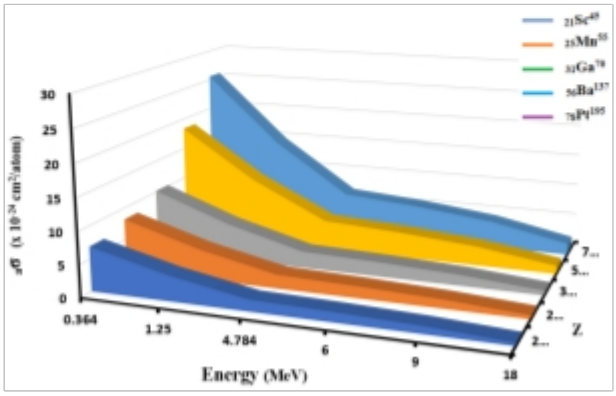

Figure 2) *Variation in the Klein-Nishina atomic cross-section as a function of E and Z.*

Figure 3 shows how the compton mass attenuation coefficient (σ/ρ) durin gth eradiation interaction with the investigated materials changes when the Klein-Nishina electronic cross-section and the ratio of charge number to mass number (Z/A) of the elements. The figure shows that σ/ρ slowly increases linearly as Z/A increases. This effect can be explained because nuclear stability demands that A increases according to Z to keep a balance between the number of protons, neutrons, and electrons in an atom. If we keep A moving proportionally to Z, then an increase in Z/A means Z is increasing slowly. If the Z effect increases, more electrons may be available to attenuate the photon beam, making the compton mass attenuation coefficient high.

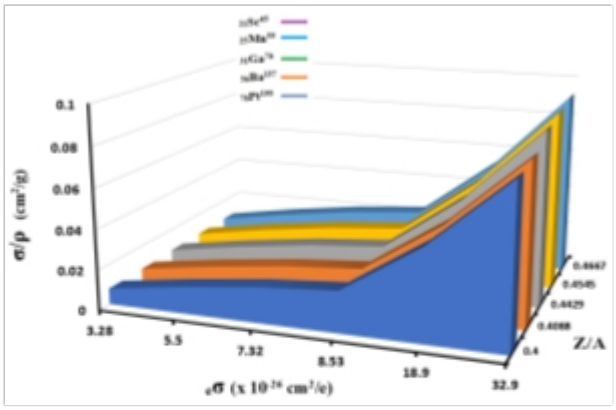

Figure 3) *Variation in the compton mass attenuation coefficient as a function of Klein-Nishina electronic cross-section and charge number to mass number ratio (Z/A) of the elements.*

This effect can be further explained based on the stability requirements of a nucleus and atom and the trend of the ratio of Z and A for that stability. Experimental results show that naturally only those nuclei and atoms are more stable for which the ratio of neutrons to protons (N/Z) varies between 1 and 1.52, except for $_1H^1$ where there are no neutrons [33-35]. This information enables us to calculate the Z/A condition of nuclear or elemental stability, which is given below.

The condition for the nuclei or elements' stability is $1 \leq N/Z \leq 1.52$.

For $N/Z = 1 \Rightarrow N = Z$. Since $A = N + Z \Rightarrow A = Z + Z = A = 2Z \Rightarrow Z/A = 0.5$

For $N/Z = 1.52 \Rightarrow N = 1.52Z$. Thus, $A = N + Z = 1.52Z + Z = 2.52Z$, which gives $Z/A = 1 / 2.52$

$\Rightarrow Z/A = 0.39$.

This calculation specifies the condition of Z/A for stable elements in nature and reveals that for stable elements $0.39 \leq Z/A \leq 0.5$.

From these facts and calculations, we can easily conclude that the Z/A of elements does not vary randomly, but rather it varies in a way to satisfy the $0.39 \leq Z/A \leq 0.5$ conditions of stability. In a nutshell, we can say that σ/ρ does not depend on Z and A independently, but rather it varies with the ratio of the two, and the range of variation is limited for stable elements. These limitations impose the condition that σ/ρ varies slowly with Z/A, as the range of Z/A is limited and restricted. Table 3 gives data and detailed values of the compton mass attenuation coefficient.

TABLE 3
Compton mass attenuation coefficients (σ/ρ) as a function of photon energy.

E (MeV)	Scandium σ/ρ (cm2/g)	Manganese σ/ρ (cm2/g)	Gallium σ/ρ (cm2/g)	Barium σ/ρ (cm2/g)	Platinum σ/ρ (cm2/g)
0.364	0.0923065	0.08989351	0.0875992	0.08085472	0.0791142
1.25	0.05304175	0.05165519	0.05033682	0.04646126	0.04546111
4.784	0.02397391	0.02334721	0.02275133	0.02099964	0.0205476
6	0.02057115	0.0200334	0.01952209	0.01801904	0.01763115
9	0.0154608	0.01505664	0.01467235	0.01354269	0.01325117
18	0.00921749	0.00897654	0.00874744	0.00807395	0.00790014

Figure 4 represents the Klein-Nishina energy transfer cross-section per electron (σ_e^{tr}) for various energy X-ray photons interacting with the investigated elements. The Klein-Nishina energy-transfer cross section per electron is the average fraction of the incident photon energy transferred to compton electrons per electron in the material traversed. The figure shows that σ_e^{tr} decreases as the energy of the incident X-ray or γ-ray increases in the 0.364 MeV to 18 MeV energy range. This means that a low-energy X-ray or γ-ray photon transfers more energy to an electron, while a low fraction of energy is transferred to the electron by a highly energetic photon during its interaction.

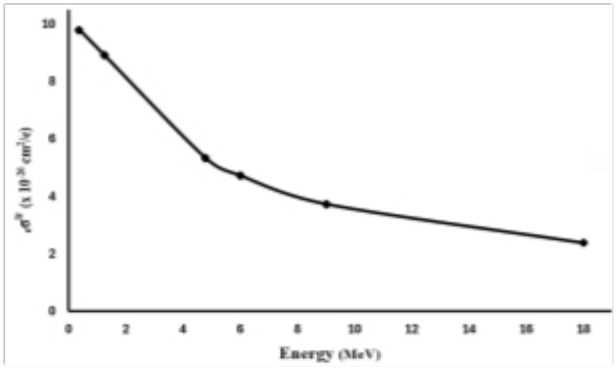

Figure 4) *Changes in the* σ_e^{tr} *with increasing X-ray or γ-ray energy.*

The reason for this behavior is the fact that low-energy photons dominantly interact by the photoelectric absorption process, in which an interacting X-ray transfers all its energy to the electron. On the other hand, compton scattering is the dominant interaction process at intermediate and high energies, followed by pair production [21,24,27]. In the compton scattering process, the photon does not transfer all its energy to the interacting electron. Instead, it transfers only a part or a fraction of its energy. Since a relatively lower fraction of the photon energy is transferred by a high-energy photon due to compton scattering, therefore, the σ_e^{tr} decreases with increasing photon energy. In general, the higher the incident photon energy, the greater the penetration depth achieved by the photon, which in turn indicates a reduction in the Klein-Nishina energy transfer cross-section per electron. The numeric values of σ_e^{tr} are given in Table 2.

Figure 5 describes how the Klein-Nishina energy transfer cross-section per atom changes when the energy of interacting radiation and the charge number Z of the atom are changed. The figure provides information about variation in with X-ray or γ-ray energy in the 0.364 to 18 MeV energy range and the charge number Z of $_{21}Sc^{45}$, $_{25}Mn^{55}$, $_{31}Ga^{70}$, $_{56}Ba^{137}$, and $_{78}Pt^{195}$. The $_a\sigma^{tr}$ provides information about the probability that an x-ray or a γ-ray photon will transfer energy to the interacting atom. Since each atom has Z electrons, for each atom may be calculated

by multiplying with the charge number Z of the atom. Figure 5 shows that Platinum (Pt-195), with Z=78, has a higher energy transfer cross-section per atom due to its higher Z. As the number of electrons, which is expressed in terms of Z, increases, the chance of transferring energy increases. This is because a photon may have more chances of interacting with and scattering from many electrons of the interacting atom, thereby losing more energy. As photon energy increases within the scattering range, the chances of compton scattering also increase, and the interacting photon retains a high amount of energy instead of transferring more energy to the interacting atom as occurs in photoelectric absorption. Thus, the probability of transferring energy decreases as the energy of the photon increases. At 12 MeV and 18 MeV energies, the cross-section is very low due to pair production occurring readily at these energies.

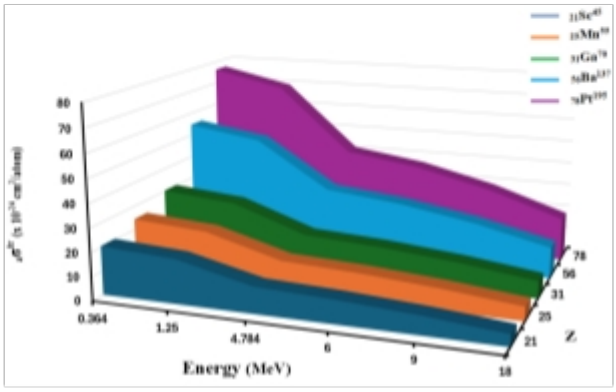

Figure 5) *Variation in the Klein-Nishina energy transfer cross-section per atom* (σ_a^{tr}) *as a function of radiation energy e and charge number z of the elements.*

Figure 6 provides information about variation in compton mass-energy transfer coefficient ($\boldsymbol{\sigma}^{tr}/\rho$) as a function of the energy of radiation (E), and the charge number (Z) of the elements. As the photon energy increases within the scattering range, the chances of compton scattering increase; however, at high energies, the photon retains lots of its energy with a low chance of transferring its energy as in the scattering process. This retaining of its energy and not transferring big energy to the atom by compton scattering makes the photon mostly move forward in the compton scattering [36-38]. Thus, the probability of transferring energy by the mechanism of scattering decreases as the energy of the photon increases. The value of σ^{tr}/ρ varies slowly with the charge number Z. The figure shows that σ^{tr}/ρ decreases slowly as Z increases.

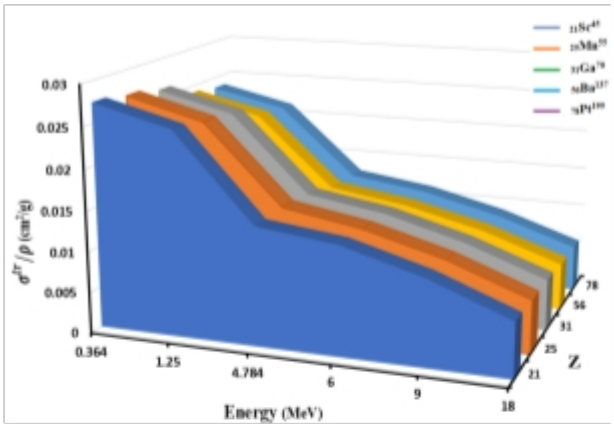

Figure 6) *Variation in the compton mass-energy transfer coefficient (σ^{tr}/ρ) as a function of the radiation energy (E), and the charge number (Z) of the elements.*

This behavior can be explained based on the fact that σ^{tr}/ρ is the coefficient of fractional energy that is transferred to the electron during compton scattering of an X-ray or γ-ray photon, and it is not just the probability of occurrence of compton scattering. This behavior provides us the information that σ^{tr}/ρ may not have a simple relationship with Z. Since changes in Z are also accompanied by changes in A for a stable nucleus, therefore, it is difficult to find a relationship between σ^{tr}/ρ and Z independent of A. Thus, in studying σ^{tr}/ρ as a function of the nature of an atom, both Z and A should be taken into consideration as a single entity, like the ratio of Z and A, instead of Z and A being separate from each other. Table 4 gives further details about the compton mass-energy transfer coefficient.

TABLE 4
Compton mass-energy transfer coefficient at various photon energies.

E (MeV)	Scandium (σ/ρ) tr (cm2/g)	Manganese (σ/ρ)tr (cm2/g)	Gallium (σ/ρ)tr (cm2/g)	Barium (σ/ρ)tr (cm2/g)	Platinum (σ/ρ)tr (cm2/g)
0.364	0.0275	0.0268	0.0261	0.0241	0.0236
1.25	0.025	0.0243	0.0237	0.0219	0.0214
4.784	0.0145	0.0146	0.0142	0.0131	0.0128
6	0.0133	0.0146	0.0126	0.0116	0.0114
9	0.0105	0.0102	0.0099	0.0092	0.009
18	0.0067	0.0065	0.0063	0.0058	0.0057

Conclusion

The Klein-Nishina electronic and atomic cross-sections and compton coefficients, investigated for $_{21}Sc^{45}$, $_{25}Mn^{55}$, $_{31}Ga^{70}$, $_{56}Ba^{137}$, and $_{78}Pt^{195}$, using X-ray energies ranging from 0.364 MeV to18 MeV are found to be decreasing while the X-ray energy increases. This behavior informs us that in all applications where scattering is needed, lower energy photons should be used, and to avoid scattering, photon energy above 10 MeV should be the choice. The electronic and atomic cross-sections seem to increase for high-Z materials, while compton coefficients are more dependent on the Z/A ratio of materials instead of Z o r Aseparately. This work provides information about the type of material one should use in various applications, like choosing radiation shielding material and dose calculation, and correction during radiological and therapeutic applications of radiation. The work also concludes that the use of a shielding material and knowing about the compton scattering coefficients can improve radiological imaging quality by controlling the intensity and energy of X-rays.

References

1. Dunn J. It is time to close the gap in cancer care. JCO Glob Oncol. 2023;9:e2200429.

2. Bray F, Laversanne M, Sung H, et al. Global cancer statistics 2022: GLOBOCAN estimates of incidence and mortality worldwide for 36 cancers in 185 countries. CA Cancer J Clin. 2024;74:229-63.

3. Mould RF. Röntgen and the discovery of X-rays. Brit J Radiol. 1995;68:1145-76.

4. Brenner DJ, Doll R, Goodhead DT, et al. Cancer risks attributable to low doses of ionizing radiation: assessing what we really know. Proc Natl Acad Sci. 2023;100:13761-6.

5. Donya M, Radford M, El Guindy A, et al. Radiation in medicine: origins, risks and aspirations. Glob Cardiol Sci and Practi. 2015;2014:57.

6. Preston DL, Shimizu Y, Pierce DA, et al. Studies of mortality of atomic bomb survivors. Report 13: solid cancer and noncancer disease mortality: 1950–1997. Rad Rec. 2003;160:381-407.

7. Land CE. Estimating cancer risks from low doses of ionizing radiation. Sci. 1980;209:1197-203.

8. Hopkins DN, Maqbool M, Islam MS. Linear attenuation coefficient and buildup factor of MCP-96 alloy for dose accuracy, beam collimation, and radiation protection. Rad Phys Tech. 2012;5:229-36.

9. Harrison JD, Haylock RG, Jansen JT, et al. Effective doses and risks from medical diagnostic x-ray examinations for male and female patients from childhood to old age. J Rad Protect. 2023;43:011518.

10. Peet DJ, Morton R, Hussein M, et al. Radiation protection in fixed PET/CT facilities-design and operation. Brit J Radiol. 2012;85:643-6.

11. Erdman M, King S, Miller K. Recent experiences with shielding a PET/CT facility. Health Phys. 2004;87:S37-9.

12. Alenezi A, Soliman K. Trends in radiation protection of positron emission tomography/computed tomography imaging. Ann ICRP. 2015;44:259-79.

13. AbuAlRoos NJ, Amin NA, Zainon R. Conventional and new lead-free radiation shielding materials for radiation protection in nuclear medicine: a review. Radiat Phys and Chem. 2019;165:10843-9.

14. Williams KA, Wright BK, Perrigin MW, et al. Radiation shielding characterization of $_{83}Bi^{209}$, $_{74}W^{184}$, $_{50}Sn^{119}$, ZnS, and CaCO3 using the modified Klein-Nishina formula. Radiat Phys and Chem. 2023;205:1107-12.

15. Perrigin MW, Williams KA, Wright BK, et al. Low melting point MCP-69, MCP-96, MCP-137, and MCP-200 alloys for radiation protection in radiological and therapeutic processes. Radiat Med Prot. 2022;3:175-82.

16. Covens P, Berus D, Buls N, et al. Personal dose monitoring in hospitals: global assessment, critical applications and future needs. Radiat Prot Dosim. 2007;124:250-9.

17. Hyun SJ, Kim KJ, Jahng TA, et al. Efficiency of lead aprons in blocking radiation− how protective are they? Heliyon. 2016;2:e00117.

18. Shultis JK, Faw RE. Radiation shielding technology. Health Phys. 2005;88:587-612.

19. Yu H, Tang X, Wang P, et al. Safety verification of radiation shielding and heat transfer for a model for dry. Nucl Eng Des. 2015;291:287-94.

20. Li Q, Wei Q, Zheng W, et al. Enhanced radiation shielding with conformal light-weight nanoparticle–polymer composite. ACS appl mater interfaces. 2018;10:35510-5.

21. Hirayama H, Nakashima H, Morishima M, et al. Progress and prospects of calculation methods for radiation shielding. J Nucl Sci Technol. 2015;52:1339-61.

22. Baltas H, Celik S, Cevik UG, et al. Measurement of mass attenuation coefficients and effective atomic numbers for MgB2 superconductor using X-ray energies. Radiat Meas. 2007;42:55-60.

23. Akca B, Erzeneoglu SZ. The mass attenuation coefficients, electronic, atomic, and molecular cross sections, effective atomic numbers, and electron densities for compounds of some biomedically important elements at 59.5 keV. Sci Technol Nucl Install. 2014;2014:901465.

24. Thiele KT, Alexander RW, Maqbool M, Characterization of $_{83}Bi^{209}$, $_{74}W^{184}$, $_{48}Cd^{112}$, $_{30}Zn^{65}$, $_{28}Ni^{59}$ and $_{26}Fe^{56}$ using Modified Klein-Nishina formula, for radiation shielding and dosimetry. Radiat Phys Chem. 2001;179:109264.

25. Yorke E, Gelblum D, Ford E. Patient safety in external beam radiation therapy. Am J Roentgenol. 2011;196:768-72.

26. Holmberg O, Czarwinski R, Mettler F. The importance and unique aspects of radiation protection in medicine. Eur J Radiol. 2010;76:6-10.

27. Fatima Z, Ali N, Williams MA, et al. X-ray scattering and attenuation cross-sections and coefficients of bone, brain, lung, fat, and soft tissue for applications in dosimetry, cancer detection, and treatment. Radiat Phys Chem. 2023;208:110908.

28. Holmberg O, Czarwinski R, Mettler F. The importance and unique aspects of radiation protection in medicine. Eur J Radiol. 2010;76:6-10.

29. Karim Karoui M, Kharrati H. Monte Carlo simulation of photon buildup factors for

shielding materials in radiotherapy X-ray facilities. Med Phys. 2013;40:073901.

30. Latha P, Abdullah KK, Unnikrishnan MP, et al. Differential scattering cross sections for elements with 13 less-than-or-slanted-equal-To Z less-than-or-slanted-equal-to 50 using 59.54 keV gamma rays. Phys Scr. 2012;85:1-5.

31. Yazaki Y. How the klein–nishina formula was derived: Based on the sangokan nishina source materials. Proc Jpn Acad Ser B Phys Biol Sci. 2017;93:399-421.

32. Parvaresh R, Jalili M, Haghparast A, et al. Evaluations for determination of optimum shields in nuclear medicine. J Biomed Phys Eng. 2020;10:651.

33. Thoennessen M. Reaching the limits of nuclear stability. Rep Prog Phys. 2004;67:1187.

34. Cziraki A. Stability of nuclei based on the new proton and neutron model. Nat Sci. 2023;15:289-99.

35. G Lambrinou. Assessment of nuclear stability and Its characteristics. Mod Chem Appl. 2022;10:1000351.

36. Scannavino Jr FA, Cruvinel PE . Agraphical tool for an analytical approach of scattering photons by the compton effect. Nucl Instrum Methods Phys Res Sect A. 2012;674:28-38.

37. Jones KC, Redler G, Templeton A, et al. Characterization of compton-scatter imaging with an analytical simulation method. Phys Med Biol. 2018;63:025016.

38. Sopena A, Palacios A, Catoire F, et al. Angle-dependent interferences in electron emission accompanying stimulated compton scattering from molecules. Commu Phys. 2021;4:253.